



Optimization of components and layouts of hydromechanical transmissions

Antonio Rossetti^a , Alarico Macor^b  and Martina Scamperle^b 

^aConstruction Technologies Institute, National Research Council, Padova, Italy; ^bDepartment of Engineering and Management, University of Padua, Vicenza, Italy

ABSTRACT

In the agricultural and work machine sectors, hydromechanical transmission competes with traditional mechanical transmission. However, the double energy conversion taking place in hydrostatic transmission lowers the efficiency of the entire transmission. Thus, the dimensioning of hydromechanical transmission must not only meet the functional requirements of speed and power to be transmitted, but must also identify the particular combination of layout and the components that leads to the maximum efficiency. In this study, a general answer to this problem will be given. The design is transformed into a mathematical programming problem, whose goal is the optimisation of both the configuration and internal components of the transmission. The structure of the transmissions is described by means of graph theory, and the resolution of the optimisation problem is obtained by means of a 'direct search' algorithm based on the swarm method.

ARTICLE HISTORY

Received 24 August 2016
Accepted 15 February 2017

KEYWORDS

Hydromechanical transmission; layout optimisation; input coupled CVT; output coupled CVT

1. Introduction

The recent evolution of transmission systems for agricultural and work machinery was directed towards an improvement of comfort and drivability without loss in efficiency and, if possible, increases of costs. These objectives involve the use of continuous transmissions that allow the elimination of gear shifts, which are sometimes tiring, and the management of the engine at minimum specific consumption conditions. Hydromechanical transmission meets these requirements well, so it is increasingly installed in medium-large machines (Jarchow 1964, Kress 1968, Renius and Resch 2005).

Hydromechanical transmission transmits the power partly through a fixed ratio branch and partly through a variable ratio branch, which is made up by a hydrostatic group. A planetary gear train will add the two powers, as in the input coupled (IC) layout (Figure 1), or split them between the two branches, as in output coupled (OC) layout (Figure 2). Based on these two basic configurations, more complex structures can be derived, such as the input coupled Dual Stage and the output coupled compound (Blake *et al.* 2006) The continuous variation of output speed is obtained acting on the displacement of the two hydraulic machines.

However, the double conversion of energy in the hydrostatic units lowers the average efficiency of the entire driveline below the typical efficiency of conventional mechanical transmission.

As with all continuously variable transmissions, hydromechanical transmission separates the wheel speed from the engine speed, making it possible to manage the engine optimally. It has been shown that the optimal management of the engine produces beneficial effects greater than the negative effects induced by the transmission (Macor and Rossetti 2013).

Compared to conventional powertrains, consisting of torque converter and a power shift gearbox used in medium to heavy work machines, the hydro-mechanical transmission actually offers higher efficiency. The power shift transmission can give a slightly higher efficiency in the high-speed range, but only if the converter is locked and the gearbox has relatively few gear stages. The major difference between these two transmission concepts is that the torque converter is a self-adjustable unit, which gives excellent start performance and automatically prevents wheel slip. On the other hand, the hydro-mechanical transmission requires advanced active control of the hydrostatic machines to create similar performance as a torque converter. In addition to the control problems of hydro-mechanical transmission, it has also been difficult to achieve a cost-effective design that can compete with conventional powertrains.

This work attempts to overcome this difficulty.

In the literature, the design has been interrogated in various ways, which are all based on a dimensioning to meet power and speed requirements (Sung *et al.* 2005,

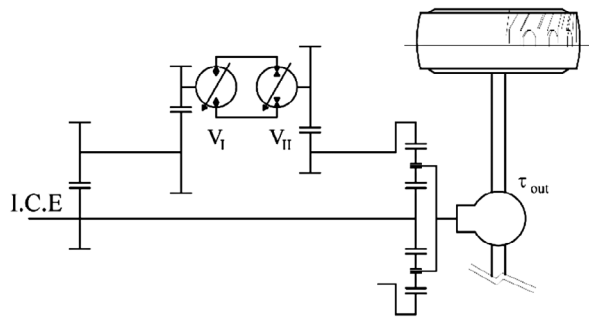


Figure 1. Schematic of the input coupled configuration.

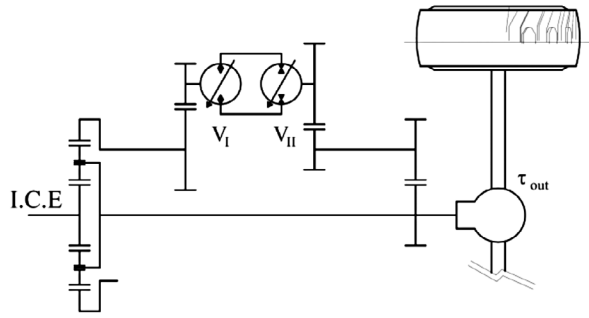


Figure 2. Schematic of the output coupled configuration.

Linares *et al.* 2010), sometimes followed by a simulation (Kirejczyk 1984, Mikeska and Ivantysynova 2002, Krauss and Ivantysynova 2004, Blake *et al.* 2006, Casoli *et al.* 2007).

A step ahead of this approach was carried out by Macor and Rossetti (2011), who considered the sizing as an optimisation problem, whose objective function to be maximised is the average efficiency of the transmission along the rated speed range of the vehicle. In contrast, for Rossetti and Macor (2013), the design is a multiobjective problem whose objective functions are the efficiency to be maximised, and the transmission bulk to be minimised.

Obviously, many other aspects should be considered in a design procedure, such as the noise. An attempt in this direction was made by Macor *et al.* (2016).

In previous studies, optimisation is applied to transmissions whose structure is assigned a priori. However, the various layouts do not have the same performance, because they have different internal power flows during operation and different internal losses. Therefore, the optimisation of transmission must also cover the layout, not only the components.

For this reason, we present an optimisation approach for the design of three-shaft hydromechanical transmissions whose goal is the simultaneous optimisation of structure and components.

The structure is implemented by means of graph theory, whereas the components are described by their functional models.

Since the problem is strongly non-linear, a direct search algorithm based on swarm theory (Particle

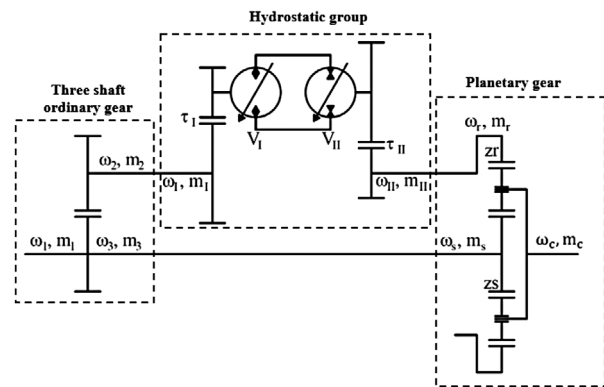


Figure 3. Schematic of power split transmission.

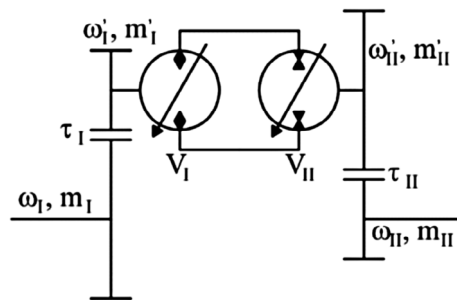


Figure 4. Schematic of the hydrostatic group.

Swarm Optimizer, PSO: Fan *et al.* 2014) is used to solve the optimisation problem.

Finally, the optimisation procedure will be applied to the transmission of a high-power agricultural tractor.

2. Model

To calculate the performance of power split transmission, two different approaches can be used: stationary and time-variant. For a model to be coupled to an optimizer, the former seems to be more suitable, because it is faster, provided that the efficiency of the hydraulic machines is not considered as constant. The model adopted here has these features.

The schematic of a generic transmission is illustrated in Figure 3, whose main groups will be discussed below.

2.1. Hydrostatic group

The hydrostatic group is the continuously variable element of power split transmission. It is made up by two variable-displacement reversible hydraulic machines (Figure 4).

By varying the two displacements, it is possible to vary the transmission ratio continuously. Two gears τ_I and τ_{II} are added to fit the input and output speeds to the operating range of the hydrostatic units.

The fundamental equations regulating the power transmission inside the unit in Figure 3 are the continuity equation and the uniqueness of the pressure drop

of the two machines, which is derived from the equation of the torques.

The ratios τ_I and τ_{II} will be defined as follows:

$$\begin{aligned}\omega'_I &= \tau_I \omega_I \\ \omega'_{II} &= \tau_{II} \omega_{II}\end{aligned}\quad (1)$$

$$\left[\tau_I \alpha_I V_I \eta_{vI}^k - \tau_{II} \alpha_{II} V_{II} \eta_{vII}^{-k} \right] \begin{Bmatrix} \omega_I \\ \omega_{II} \end{Bmatrix} = 0 \quad (2)$$

$$\left[\frac{(\eta_{hym I} \eta_{gear}^{nI})^k}{\tau_I \alpha_I V_I} - \frac{(\eta_{hym II} \eta_{gear}^{nII})^{-k}}{\tau_{II} \alpha_{II} V_{II}} \right] \begin{Bmatrix} m_I \\ m_{II} \end{Bmatrix} = 0 \quad (3)$$

where the fractional displacement α changes from -1 to 1 for IC layout, and from 0 to 1 for OC layout. The exponent k is a function of the power flow direction; in particular, $k = 1$ if the power goes from I unit to II unit; $k = -1$ in the opposite case; the efficiencies η_v and η_{hym} are, respectively the volumetric and hydromechanical efficiency of units I and II, whereas η_{gear} takes into account the mechanical losses in the ordinary gears. The exponents n_I and n_{II} represent the number of gear pairs needed to achieve the gear ratio τ_I and τ_{II} ; they are estimated on the basis of τ_{max} , the maximum allowable value for each gear pair:

$$n_I = \text{int}(\tau_I / \tau_{max}) \quad (4)$$

$$n_{II} = \text{int}(\tau_{II} / \tau_{max})$$

2.2. Mechanical elements

The main mechanical elements inside power split transmission are the three-shaft ordinary gear (Figure 5(a)), and the planetary gear, which is the summation point of the three shafts speed (Figure 5(b)).

The kinematic and dynamic equations of the three-shaft ordinary gear are:

$$\begin{bmatrix} 1 & 0 & -1 \\ 1 & 1 & 0 \end{bmatrix} \begin{Bmatrix} \omega_1 \\ \omega_2 \\ \omega_3 \end{Bmatrix} = 0 \quad (5)$$

$$\begin{bmatrix} 1 & -1 & 1 \end{bmatrix} \begin{Bmatrix} m_1 \\ m_2 \\ m_3 \end{Bmatrix} = 0 \quad (6)$$

In which the transmission ratio was assumed to be equal to one, because speed reductions or multiplication can be incorporated in the τ_I and τ_{II} gears of the

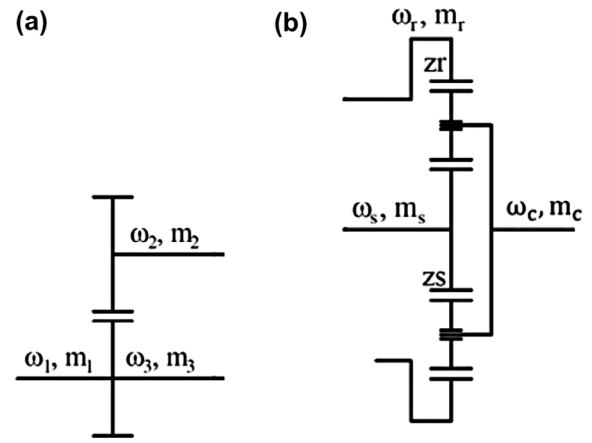


Figure 5. Schematic of the three-shaft ordinary gear (a) and the planetary gear (b).

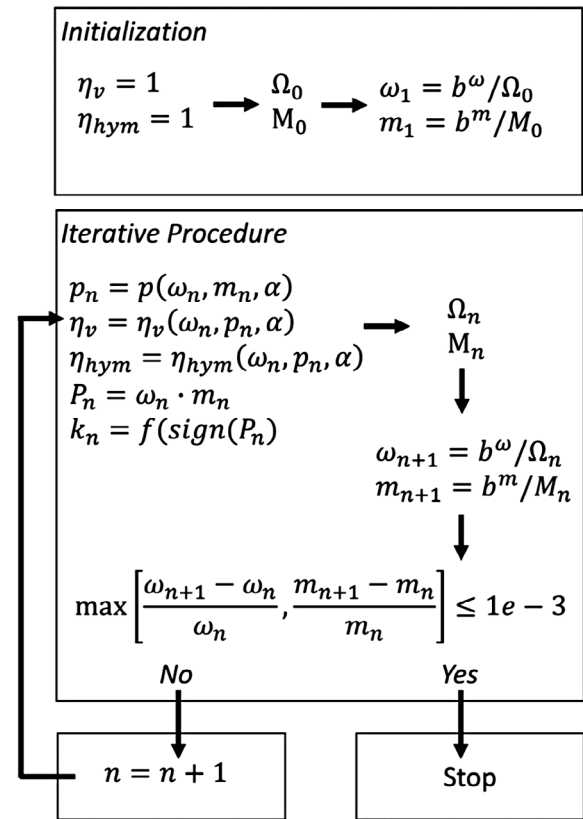


Figure 6. Flowchart of the iterative procedure for the resolution of the system.

CVT element. The velocity and torque equations of the planetary gear are:

$$\begin{bmatrix} (1-T) & -1 & +T \end{bmatrix} \begin{Bmatrix} \omega_c \\ \omega_r \\ \omega_s \end{Bmatrix} = 0 \quad (7)$$

$$\begin{bmatrix} 1 & (1-T\eta_0^{-t}) & 0 \\ 0 & T\eta_0^{-t} & 1 \end{bmatrix} \begin{Bmatrix} m_c \\ m_r \\ m_s \end{Bmatrix} = 0 \quad (8)$$

where T is the standing transmission ratio and η_o is the efficiency of the planetary gearing.

The exponent t can take ± 1 values and depends on the power flow inside the gear. The values of t can be synthetically expressed as a function of the incoming power of the sun gear, measured in relative reference to the carrier: $t = \text{sign}\left([m_s(\omega_s - \omega_c)]\right)$.

2.3. Overall system of equations

The Equations (5)–(8) define a system of six equations and twelve unknowns. The missing equations are the relationships linking the elements of the transmission: in such a way they define the transmission structure. These equations require the equality of speed and the equilibrium of the moments between the internal organs of the transmission. In the case of transmission in Figure 3, these are:

$$\begin{cases} \omega_3 - \omega_s = 0 \\ \omega_2 - \omega_I = 0 \\ \omega_r - \omega_{II} = 0 \end{cases} \quad (9)$$

$$\begin{cases} m_3 + m_s = 0 \\ m_2 + m_I = 0 \\ m_r + m_{II} = 0 \end{cases} \quad (10)$$

The final constraints are the speed and the torque of the engine at the input shaft. For example, for the case in Figure 3, the constraints $\omega_1 = \omega_{\text{engine}}$ and $m_1 = m_{\text{engine}}$ allow a determined system of fourteen equations and fourteen unknowns.

The model can be summarised in matrix form as follows:

$$\begin{aligned} \Omega \cdot \vec{\omega} &= b_\omega \\ M \cdot \vec{m} &= b_m \end{aligned} \quad (11)$$

Alternatively, the equations can be grouped into three classes: the elements, the links between elements, and the links with the outside. Therefore, the system takes the modular form:

$$\begin{aligned} \begin{bmatrix} \Omega_{\text{elements}} \\ \Omega_{\text{links}} \\ \Omega_{\text{engine}} \end{bmatrix} \cdot \vec{\omega} &= \begin{bmatrix} 0 \\ \vdots \\ \omega_{\text{engine}} \end{bmatrix} \\ \begin{bmatrix} M_{\text{elements}} \\ M_{\text{links}} \\ M_{\text{engine}} \end{bmatrix} \cdot \vec{m} &= \begin{bmatrix} 0 \\ \vdots \\ m_{\text{engine}} \end{bmatrix} \end{aligned} \quad (12)$$

The strong non-linearity of the efficiency of the hydraulic units prevents the direct resolution of the system.

Consequently, an iterative resolution was used, in which the efficiencies at the first iteration were set equal to one. The convergence criterion was assumed to be equal to 0.1% between two successive iterations. A flowchart of the iterative scheme is represented in Figure 6.

3. Optimisation

The simulator was inserted into an optimisation procedure that allows simultaneous optimisation of both the internal components and the structure of the transmission. The optimisation procedure can be formulated in this general form:

Find $x = [x_1 \ x_2 \ \dots \ x_n]^T$ minimising $f(x)$;
subject to the constraints $g_j(x) \leq 0 \ j = 1 \dots m$ and $l_j(x) = 0 \ j = 1 \dots p$.

where:

- $x_1 \ x_2 \ \dots \ x_n$ are the free optimisation variables (degrees of freedom);
- the equality constraints $l_j(x) = 0 \ j = 1 \dots p$ are the design parameters;
- the inequality constraints $g_j(x) \leq 0 \ j = 1 \dots m$ are the design constraints; and
- $f(x)$ is the objective function.

3.1. Degrees of freedom

The variables of the optimisation can be divided into two groups: variables linked to the transmission structure and component variables. The latter are:

- the displacements V_I and V_{II} ;
- the transmission ratios τ_I and τ_{II} ;
- The standing transmission ratio T of the planetary gear;
- The transmission ratio τ_{out} of the gears (both ordinary and planetary) between the output shaft of the power split transmission and the wheel axis.

Since the transmission structure can be represented in matrix form, as seen from Equations (11) and (12), the variables associated with the layout of the transmission are:

- the internal relationships of the transmission Ω_{links} ;
- the connection between the transmission and the engine Ω_{engine} .

These two variables were assembled in a unique matrix completely defining the transmission layout.

$$\Omega_{\text{layout}} = \begin{bmatrix} \Omega_{\text{link}} \\ \Omega_{\text{engine}} \end{bmatrix}$$

3.2. Design parameters

The design parameters supplied as input to the optimisation procedure are:

- internal combustion engine (ICE) design power (generally close to the best efficiency power);
- design speed of ICE;
- maximum speed of the vehicle;
- maximum wheel pulling force;
- wheel radius.

3.3. Design constraints

The optimisation procedure must be forced to satisfy some design and structural constraints. In particular:

- maximum pressure of hydraulic machines: $\Delta p \leq \Delta p_{\max}$;
- minimum and maximum transmission ratios of the planetary gear: $T_{\min} \leq T \leq T_{\max}$
- maximum and minimum volume allowed for the units displacement: $V_{\min} \leq V_I$ and $V_{II} \leq V_{\max}$;
- maximum speed of hydraulic units as a function of displacement: ω'_I and $\omega'_I \leq \beta(\alpha) \omega_{\max}(V)$.

The maximum speed of the hydraulic units was considered a function of the nominal displacement, $\Omega_{\max}(V)$. Because the maximum speed of the units refers to the full displacement condition, an overspeed factor $\beta(\alpha)$ was added to model the increase of the maximum speed in the partial displacement conditions ($\alpha < 1$).

The constraints were implemented according to penalty functions, which add a quantity proportional to the exceeded distance from the allowed domain.

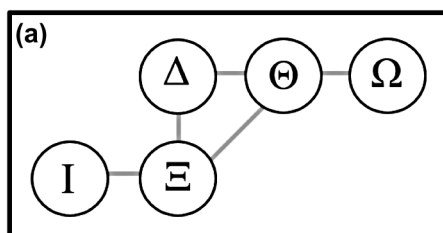
3.4. Objective function

The objective function is the integral average loss calculated between the zero speed and maximum design speed of the vehicle:

$$f(x) = P_{\text{loss}} = \frac{1}{v_{\max}} \int_0^{v_{\max}} (1 - \eta_{\text{drive line}}) P_{\text{eng}} dv \quad (13)$$

where $\eta_{\text{drive line}}$ is the transmission efficiency, defined as the ratio between the power delivered at the wheels and the engine power:

$$\eta_{\text{drive line}} = \frac{P_{\text{wheel}}}{P_{\text{engine}}} \quad (14)$$



4. Optimisation algorithm

The optimisation of the system was structured according to a hierarchical logic, by dividing the structural variables (i.e. Ω_{links} and Ω_{engine}) from the internal variables. This need comes from the lack in continuity and order of the set of the possible structures of a transmission. In fact, while the optimisation of internal parameters is possible via classical algorithms or a direct-type search, the lack of an order relation between the possible values of Ω_{links} and Ω_{engine} does not allow the definition of the sum, or other algebraic operations on which are based all the advanced optimisation algorithms.

Given that the set of configurations is finite, it is still possible to proceed to the optimisation via the enumeration of the possible configurations. Therefore, the optimisation develops according to the following scheme.

All the possible configurations of three-shaft transmission are initially defined; for each of these configurations, a process of optimisation of the internal variables is carried out, in order to obtain the value of the local optimum of that configuration. Finally, the global optimum is obtained by considering the best value among the local optima identified.

4.1. Definition of the possible configurations

In order to enable an effective enumeration and storage of the possible configurations, an abstract representation based on the graph theory was used.

A graph is a mathematical structure consisting of nodes connected by arcs. In the case in hand, the nodes represent the transmission elements such as a pump, motor planetary gear, etc.; and the arcs represent the shafts. The number of arcs that connect to a node is called the degree of the node. Five nodes were identified:

- 1 node – degree 2; the CVT variator, represented by the symbol Δ ;
- 2 nodes – degree 3; ordinary gear (symbol Ξ) and planetary gear (symbol Θ)
- 2 nodes – degree 1; transmission input (I) and output (Ω).

Following this nomenclature, IC and OC transmissions can be represented as shown in Figure 7.

The definition of the possible graphs was obtained with the following steps:

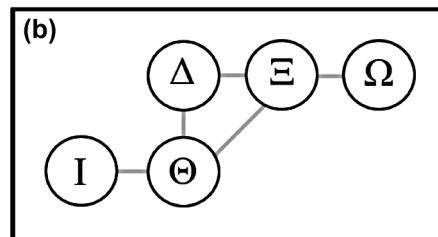


Figure 7. Base graph for the IC configuration (a) and OC configuration (b).

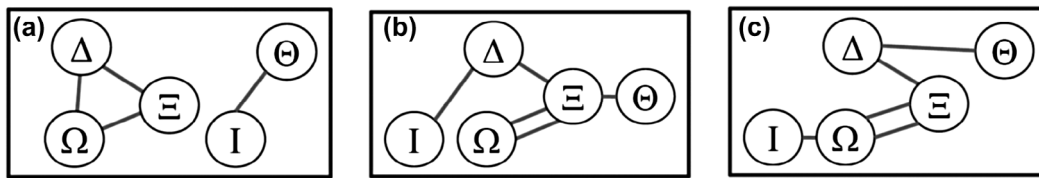


Figure 8. Graphs physically not acceptable or not significant.

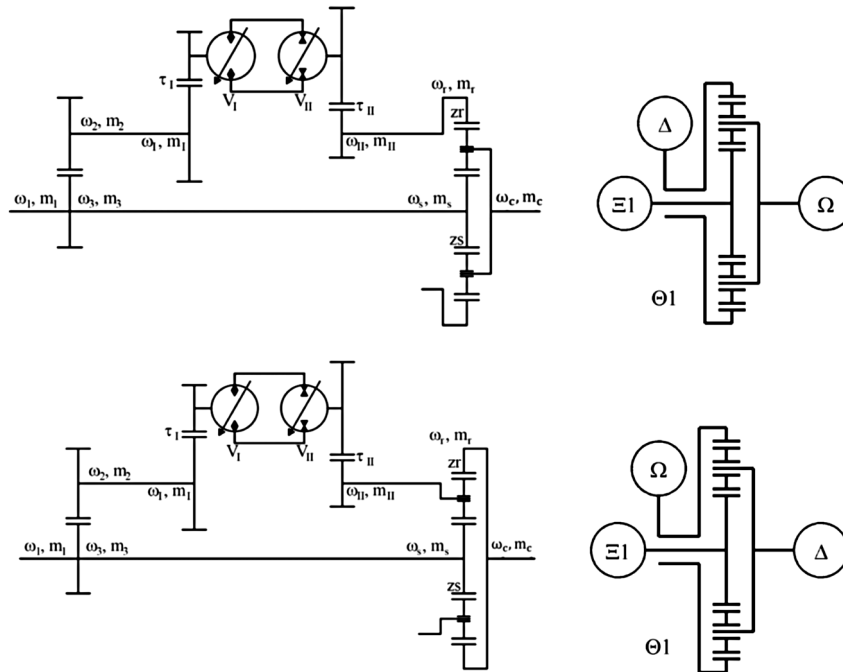


Figure 9. Different layouts for IC configuration and their representations.

- (1) Identification of possible graphs;
- (2) Removal of meaningless graphs (Figure 8), such as:
 - (a) physically undetermined graphs (Figure 8(a));
 - (b) mechanically wrong (when CVT is connected to an input or an output: Figures 8(b) and (c))

This procedure obtained a known, but nontrivial, result: the only meaningful graphs for a three-shaft layout are IC and OC of Figure 7.

In searching for the possible graph configurations, the asymmetry of the shafts of the epicyclic gear must be taken into account. Therefore, together with the graphs of Figure 7, many other combinations must be considered. By way of example, Figure 9 shows two possible configurations of the base graph of IC, which differ by the connections of the planetary gear.

Since we consider three-shaft planetary gears, the number of possible permutations of the connection with the remaining elements is six. It follows that any graph generates $6^{n_{\text{epi}}}$ configurations, where n_{epi} is the number of planetary gears in the transmission. Therefore, graphs of

the possible configurations are six for the IC graph based and six for the OC graph based.

4.2. Optimizer for continuous variables

Because the objective function of the optimisation is not directly expressed through an analytical formulation, it was decided to resort to optimisation algorithms of the direct-search type. Among these, evolutionary algorithms are particularly interesting, because they are able to avoid local minima.

Search algorithms based on swarms (Particle Swarm Optimizer: PSO) are stochastic, based on the social behaviour of bird flocks and insects swarms, in which the individual information and the sharing of this information with other individuals leads to many evolutionary advantages, including improved efficiency in the search for food.

The optimizer used here, originally presented by Fan *et al.* (2014), combines the classical formulation of PSO with the Nelder–Mead algorithm (Nelder and Mead 1965). This formulation improves the efficiency of local convergence, keeping the research capabilities of the algorithm unchanged. Such an algorithm was

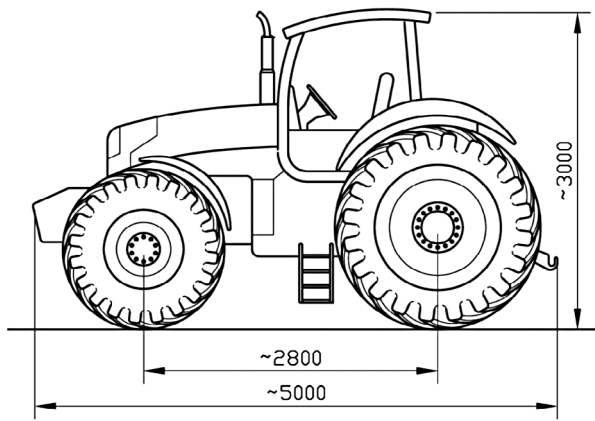


Figure 10. Overall dimensions of the tractor.

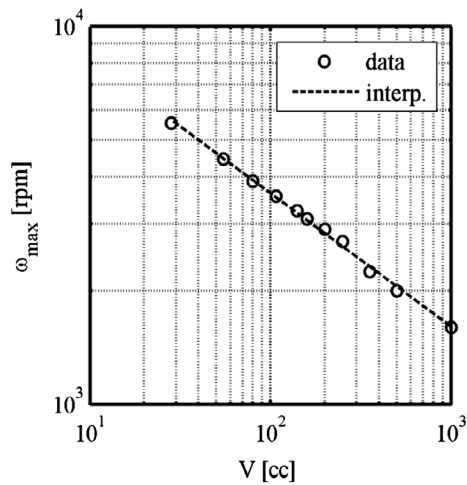


Figure 11. Maximum speed at maximum displacement as a function of the displacement (Bosch-Rexroth 2009).

successfully applied to hydromechanical transmission optimisation problems by Macor and Rossetti (2011).

5. Optimisation procedure application

The optimisation procedure previously discussed was implemented in MATLAB and applied to the transmission for a high-power agricultural tractor. The overall dimensions and the main data of the vehicle are shown, respectively in Figure 10 and Table 1. The optimisation constraints are summarised in Table 2 and Figures 11 and 12. The overspeed factor β depicted in Figure 12 is only valid for bent axis units; for swashplate units β is equal to one.

In order to contain the size of the volumetric machines, given the high value of the traction force at zero velocity, a two-speed gearbox downstream of the CVT transmission was adopted. Its gear ratio was assumed to be 4:1 in lower gear and 1:1 in higher gear. The gear shift was carried out when the transmission efficiency in second gear was higher than that of the first gear.

$$\eta_{\text{Driveline}}^{1\text{st gear}}(v_{\text{change}}) = \eta_{\text{Driveline}}^{2\text{st gear}}(v_{\text{change}}) \quad (15)$$

Table 1. Main data of the agricultural tractor.

ICE power	180 kW
ICE rated speed	2200 rpm
Wheel radius	0.965 m
Maximum traction force	120 kN
Maximum speed	40 km/h

Table 2. Optimisation constraints.

		Min	Max
Hydrostatic group			
Displacement	V	28 cc/rev	250 cc/rev
Pressure	Δp_{max}	–	400 bar
Maximum speed		0	Figures 11 and 12
Planetary gear			
Standing gear ratio	T	–1/2	–1/7

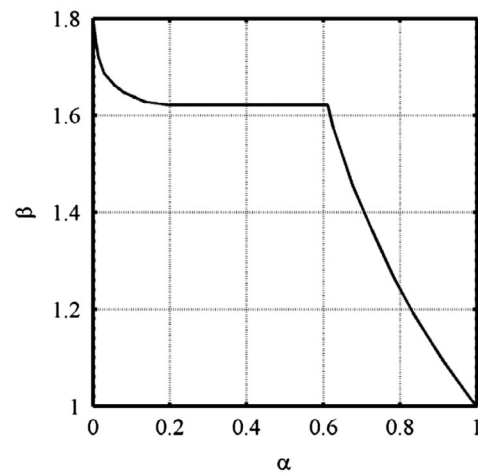


Figure 12. Increase factor of the allowable speed as a function of the partialization (Bosch-Rexroth 2009).

Consequently, the objective function is rewritten in the following form:

$$f(x) = \frac{\int_0^{v_{\text{shift}}} (1 - \eta_{\text{Driveline}}^{1\text{st gear}}) dv + \int_{v_{\text{shift}}}^{v_{\text{max}}} (1 - \eta_{\text{Drive line}}^{2\text{st gear}}) dv}{v_{\text{max}}} \quad (16)$$

As regards the efficiency laws for the hydraulic machines and the efficiency of all the gear pairs established by the model (Section 2), the following assumptions were made.

The efficiencies η_v and η_{hym} of the hydraulic machines were expressed as a function of the operating variables (Ω , α , Δp) by means of the following expressions:

$$\eta_v = \eta_{\text{ref}} \cdot \chi_{\omega}^v \left(\frac{\omega}{\omega_{\text{max}}} \right) \cdot \chi_{\alpha,p}^v \left(\alpha, \frac{\Delta p}{\Delta p_{\text{max}}} \right) \quad (17)$$

$$\eta_{\text{hy}} = \eta_{\text{ref}} \cdot \chi_{\omega}^{\text{hy}} \left(\frac{\omega}{\omega_{\text{max}}} \right) \cdot \chi_{\alpha,p}^{\text{hy}} \left(\alpha, \frac{\Delta p}{\Delta p_{\text{max}}} \right)$$

η_{ref} is the reference efficiency value, assumed to be 0.96 for both efficiencies, reduced by coefficients χ_{Ω} and

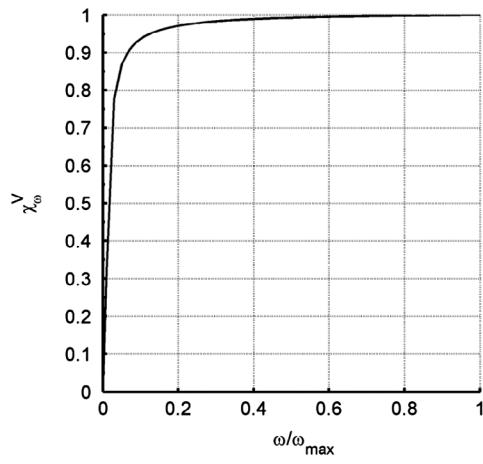


Figure 13. Effect of the speed on the volumetric efficiency.

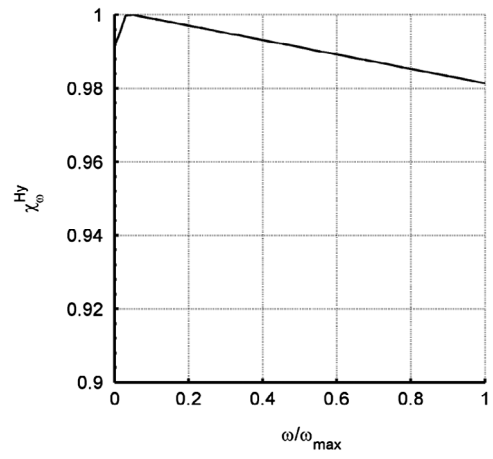


Figure 15. Effect of the speed on the hydromechanical efficiency.

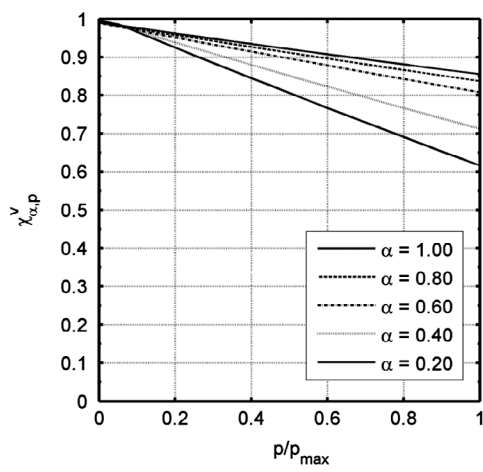


Figure 14. Effect of the pressure and displacement partialization on the volumetric efficiency.

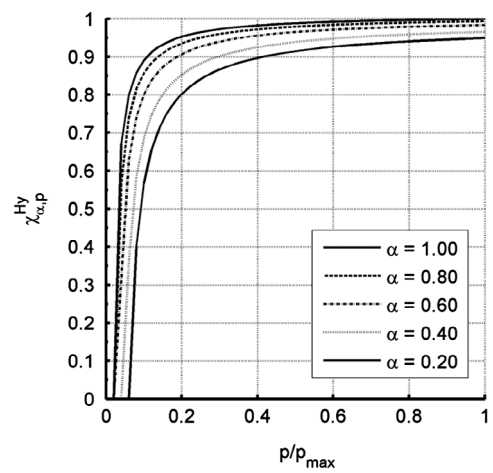


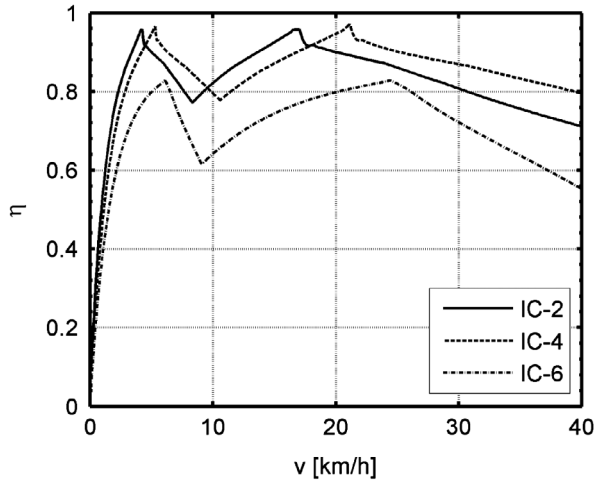
Figure 16. Effect of the pressure and displacement partialization on the hydromechanical efficiency.

Table 3. Optimal efficiencies for the IC configurations.

Input coupled	$\max(\eta_{\text{mean}})$	Input coupled	$\max(\eta_{\text{mean}})$
	[-]		.847
	.825		[-]
	[-]		.704

Table 4. Optimal values of the design variables for the IC layouts.

	IC-2	IC-4	IC-6
T	-0.15	-0.2	-0.5
V_I	28 cc/rev	54 cc/rev	244 cc/rev
V_{II}	250 cc/rev	250 cc/rev	198 cc/rev
τ_I	2.19	1.77	1.15
τ_{II}	4.0	3.90	0.72
τ_{out}	28.7	24.5	84.5
η_{mean}	0.825	0.847	0.704

**Figure 17.** Total transmission efficiency of the IC layouts.

$\chi_{\alpha,p}$. The former coefficient depends on the speed, and the latter depends on the pressure and displacement, as shown in Figures 13–16. These curves were calculated starting from the experimental curves of commercial hydraulic machines.

The efficiencies of each gear pair η_{gear} and of the planetary gear η_o were assumed to be, respectively equal to 0.985 and 0.98. The maximum gear ratio for each gear pair τ_{max} (Equation 4) was assumed to be equal to 2.

The rear axle gear was assumed to be a formed by a differential gear ($\eta = 0.975$) and by a planetary gear reducer ($\eta = 0.985$).

The full description of viscous and friction losses on the bearings, ventilation and splash oil losses of the overall transmission would lead to a very complex model. Furthermore, a detailed description of the losses requires a full description of the shafts, gears and bearings involved, which cannot be known when preliminary design considerations were drawn, as here. For this reason, the friction losses were neglected, because they do not reasonably interfere with the optimum definition, despite changing (slightly) the overall efficiency. Nevertheless, preliminary tests showed that viscous effects have a strong influence on the optimum design choice. In the absence of viscous effects, the optimum configuration will move toward a high-speed output shaft, to reduce the momentum losses on the axle gears. On the contrary, the presence of viscous effects forces the reduction of the shaft speed to a reasonable value, defining a ‘physical-based’ constraint to shaft speed.

Viscous losses were then included, using a very simple model. Because the input shaft speed is fixed and hydraulic unit’s mechanical losses were modelled inside the unit sub-system, the viscous losses on the mechanical path were considered only on the output shaft. Because the number and the disposition of the shafts of the axle gear box are not known, losses were considered, for simplicity, to come from the shaft entering the axle

Table 5. Optimal efficiencies for the OC configurations.

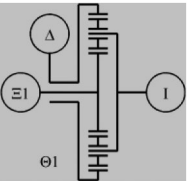
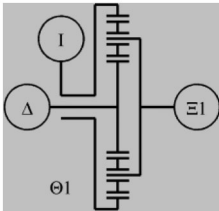
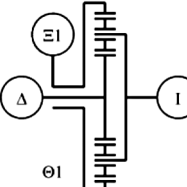
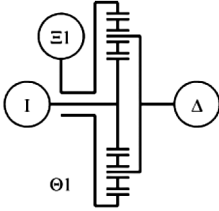
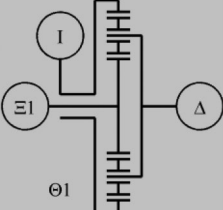
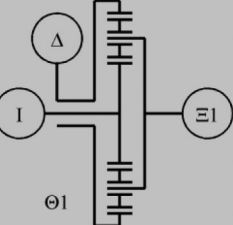
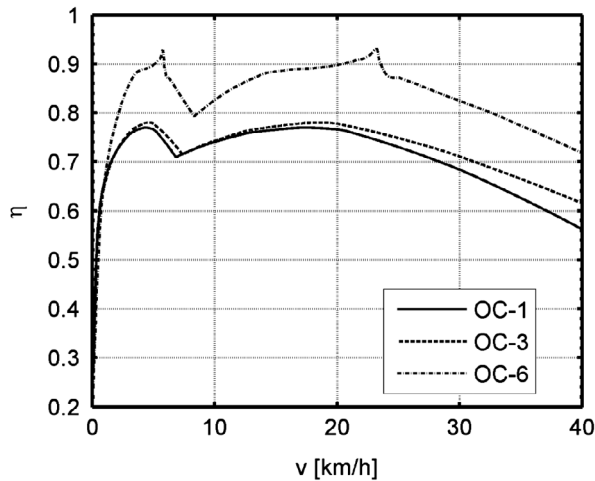
Output coupled	$\max(\eta_{mean})$	Output coupled	$\max(\eta_{mean})$
	.708		[-]
	[-]		[-]
	.682		.770

Table 6. Optimal values of the design variables for the OC layouts.

	OC-1	OC-3	OC-6
T	-0.5	-0.5	-0.5
V_I	250	250	205 cc/rev
V_{II}	117	248	250 cc/rev
τ_I	1	1	1.04
τ_{II}	1	1.03	1.05
τ_{out}	81.3	73.8	45.7
η_{mean}	.708	.682	.770

**Figure 18.** Total transmission efficiency of the OC layouts.

gear reducer. The value of $0.10 \text{ [Nm rad}^{-1} \text{ s]}$ was shown to lead to consistent results for the considered test case.

5.1. Results

The code made it possible to evaluate all the different layouts of the IC and OC configurations. The results for the IC configuration are summarised in compact form in Table 3, while the values of the optimisation variables for the solutions are shown in Table 4; Figure 17 shows the efficiency as a function of the vehicle speed at the rated power of the engine. The same results are shown in Tables 5 and 6 and Figure 18 for the OC configuration.

First, not all layouts meet the traction requirements of the vehicle, such as the IC1, IC3 and IC5 layouts for

the IC configuration (Table 3) and OC2, OC4 and OC5 layouts for the OC configuration (Table 5).

The IC configuration reaches its maximum value of efficiency with the IC4 layout, i.e. with the CVT section connected to the ring, the sun gear connected to the ordinary gear, and the carrier connected to the output.

The best solution for the OC configuration is OC5, i.e. with the CVT section connected to the ring, the solar connected to the engine, and the carrier connected to the ordinary gear.

The efficiency of the two optimal solutions is compared in Figure 19 along with that of the hydrostatic group.

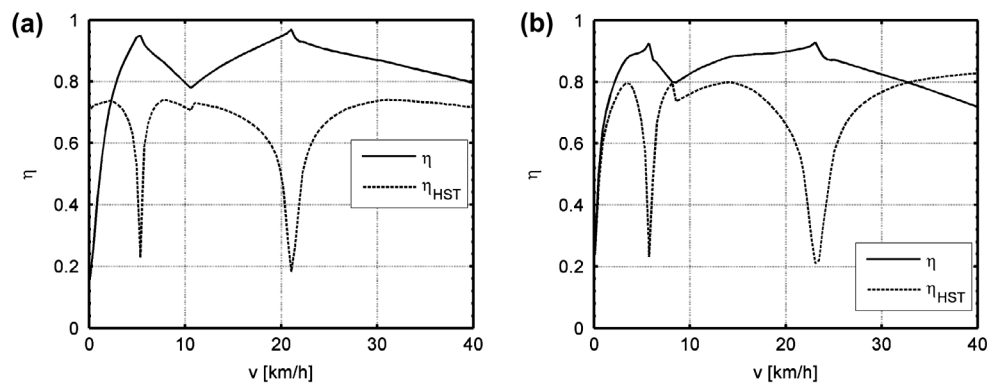
The IC superiority is not only due to the intrinsic qualities of the transmissions: actually, as shown in Figure 19, the hydrostatic group of the IC configuration, which is the main source of losses, has a lower efficiency than that of OC. This means that there must be other losses outside the transmission. These are the viscous losses in the output shaft. In fact, the transmission ratio τ_{out} of the OC solution is greater than that of the IC solution; this means that the speed of the output shaft is higher for the OC; consequently the losses will also be higher, which vary with Ω^2 .

Incidentally, the optimal displacements in Tables 4 and 6 are greater than those currently in use on tractors of a similar power.

The initial choice of ratios of 4:1 and 1:1 for the two-speed gearbox turns out to be consistent with the typical use of the vehicle: in fact, the transmission presents the best efficiency (greater than 85%) in the range of low speeds (4–8 km/h), typical of plowing operations on the field, and for high speeds (20–30 km/h), typical of road transport. The trend of the efficiency as a function of the speed is also significantly higher than the standards proposed by Renius and Resch (2005) for agricultural CVT transmissions.

6. Conclusions

The advantage resulting from the continuous speed variation of hydromechanical transmissions is partially reduced by their low efficiency, caused by the double

**Figure 19.** Total transmission efficiency and efficiency of the hydrostatic group; (a) optimal IC layout; (b) optimal OC layout.

energy conversion that takes place in the hydrostatic unit. Therefore, the design of hydromechanical transmission must be made with care in order to identify the most efficient solution.

In this study, the design of hydromechanical transmission has been approached as an optimisation problem, whose goal was the simultaneous optimisation of the layout and the components. This dual level of optimisation constitutes a strong element of novelty, because in traditional design, the layout is assumed a priori on the basis of prior knowledge; the size of the components, instead, is calculated based on the design data. In this way, the result of the design cannot be said to be optimal.

The problem of a mathematical representation of the configuration was treated by means of graph theory; the representation of the transmission is left to a simulator. In the models of hydraulic machines, appropriate efficiency functions were included, derived from experimental data provided by the manufacturers. The resolution of the optimisation problem was made through a 'direct search' algorithm based on the method of swarms.

The procedure of optimised design has been applied to the case of transmission of a high-power agricultural tractor. It provided as the optimum configuration the input coupled, having the carrier connected to the wheels and the ring connected to the hydrostatic group; its efficiency is slightly higher than the standards proposed in the literature.

Disclosure statement

No potential conflict of interest was reported by the authors.

Nomenclature

m	torque, Nm
n	number of iteration
p	pressure, Pa
v	velocity, m/s
z	teeth number
M	Torque matrix
P	power, W
V	maximum displacement, m ³ /rad
$T = -z_j/z_r$	standing gear ratio of the planetary gear
α	fractional displacement factor
η_v	volumetric efficiency
η_{hym}	hydromechanical efficiency
$\eta_{drive\ line}$	total transmission efficiency
τ	transmission ratio of a spur gear
Ω	angular velocity, rad/s
χ_Ω	speed effect correction factor of the hydraulic machine efficiency
$\chi_{\alpha,p}$	pressure and partialisation effect correction factor of the hydraulic machine efficiency
Ω	kinematic matrix

Superscripts and Subscripts

I	hydrostatic group inlet
II	hydrostatic group outlet
rif	maximum efficiency condition
1,2,3	referring to the three-shaft spur gear
c,s,r	carrier, sun, ring of the epicyclical gear
out	elements downstream of the transmission
wheel	wheel axis
'	refers to the hydraulic machine shaft

Notes on contributors



Alarico Macor has an MSc in mechanical engineering and a PhD in energetics from Padua University. He is an associate professor of fluid power systems and teaches in the Doctoral School of Mechatronics. Research activity: Performance and emission testing of biodiesel in boilers and on-road diesel engines. Hydraulic hybrid systems and hydro-mechanical power split transmissions; dynamic simulation of fluid power systems.



Antonio Rossetti received his Ph.D degree in Energetic from the University of Padova, Italy, in 2009, where he hold a Post-doc Researcher position for 3 years. In 2013 he moved to ITC-CNR as Researcher in the Thermo-Fluid Dynamics Branch. His main research fields are the experimental and numerical fluid dynamics.



Martina Scamperle graduated from the University of Padua in mechanical engineering in 2013. She has been a PhD student since 2016 in mechatronics and product innovation at the Department of Engineering and Management, University of Padua. Current research areas include experimental and theoretical analysis of hydrostatic transmissions, design of complex drivelines and dynamic simulation of fluid power systems.

ORCID

Antonio Rossetti  <http://orcid.org/0000-0003-0635-6748>

Alarico Macor  <http://orcid.org/0000-0003-2244-6524>

Martina Scamperle  <http://orcid.org/0000-0002-4822-6653>

References

- Blake C., Ivantysynova M., and Williams K., 2006. Comparison of operational characteristics in power split continuously variable transmissions. *In: 2006 SAE commercial vehicle engineering congress & exhibition*. SAE Technical Paper no. 2006-01-3468. Rosemont, IL.
- Bosch-Rexroth, 2009. Data sheet for Axial Piston Variable Motors RE 91604/07.09.
- Casoli P., et al., 2007. A numerical model for the simulation of Diesel/CVT Power Split transmission. *In: ICE2007 8th international conference on engines for automobiles*. SAE Technical Paper no. 2007-24-0137. Capri, Italy.

- Jarchow, F., 1964. Leistungsverzweigte Getriebe (Power split transmissions). *VDI-Z*, 106 (6), 196–205.
- Kirejczyk J., 1984. *Continuously variable hydromechanical transmission for commercial vehicle by simulation studies*. SAE Technical paper no. 845095, FISTIA congress, Vienna, Austria.
- Krauss A. and Ivantysynova M., 2004. Power split transmissions versus hydrostatic multiple motor concepts – A comparative analysis. In: *2004 SAE commercial vehicle engineering congress & exhibition*. SAE Technical Paper no. 2004-01-2676.
- Kress, J.H., 1968. *Hydrostatic power splitting transmissions for wheeled vehicles – classification and theory of operation*. SAE Technical Paper no. 680549. Warrendale, PA: Society of Automotive Engineers.
- Linares, P., Mendez, V., and Catalan, H., 2010. Design parameters for continuously variable power-split transmissions using planetaries with 3 active shafts. *Journal of terramechanics*, 47, 323–335.
- Macor, A. and Rossetti, A., 2011. Optimization of hydro-mechanical power split transmissions. *Mechanism and machine theory*, 46 (12), 1901–1919.
- Macor, A. and Rossetti, A., 2013. Fuel consumption reduction in urban buses by using power split transmissions. *Energy conversion and management*, 71, 159–171.
- Macor, A., Rossetti, A., and Scamperle, M., 2016. Prediction of sound pressure level for a dual-stage hydromechanical transmission. *International journal of fluid power*, 17 (1), 25–35.
- Mikeska D. and Ivantysynova M., 2002. Virtual prototyping of power split drives. In: *Proceedings of bath workshop on power transmission and motion control*, Bath, UK, 95–111.
- Nelder, J.A. and Mead, R., 1965. A simplex method for function minimization. *Computer journal*, 7, 308–313.
- Renius, K.T. and Resch R., 2005. *Continuously variable tractor transmissions*. ASAE distinguished lecture series. Tractor Design no. 29. Louisville, KY.
- Rossetti, A. and Macor, A., 2013. Multi-objective optimization of hydro-mechanical power split transmissions. *Mechanism and machine theory*, 62 (4), 112–128.
- Fan, S.-K.S., Liang, Y.-C., and Zahara, E., 2014. A genetic algorithm and a particle swarm optimizer hybridized with Nelder–Mead simplex search. *Computers & industrial engineering*, 50, 401–425.
- Sung, D., Hwang, S., and Kim, H., 2005. Design of hydromechanical transmission using network analysis. *Proceedings of the institution of mechanical engineers, part D: journal of automobile engineering*, 219 (1), 53–63.